



HAL
open science

Reaction pathways for the HDO of guaiacol over supported Pd catalysts: Effect of support type in the deoxygenation of hydroxyl and methoxy groups

Camila A. Teles, Priscilla Magalhaes de Souza, Raimundo C. Rabelo-Neto, Alejandra Teran, Gary Jacobs, Clara Vilela Weikert, Zuy M. Magriotis, Vinicius O. O. Goncalves, Daniel E. Resasco, Fabio Bellot Noronha

► To cite this version:

Camila A. Teles, Priscilla Magalhaes de Souza, Raimundo C. Rabelo-Neto, Alejandra Teran, Gary Jacobs, et al.. Reaction pathways for the HDO of guaiacol over supported Pd catalysts: Effect of support type in the deoxygenation of hydroxyl and methoxy groups. *Molecular Catalysis*, 2022, *Molecular Catalysis*, 523, pp.111491. 10.1016/j.mcat.2021.111491 . hal-04254286

HAL Id: hal-04254286

<https://hal.univ-lille.fr/hal-04254286>

Submitted on 22 Jul 2024

HAL is a multi-disciplinary open access archive for the deposit and dissemination of scientific research documents, whether they are published or not. The documents may come from teaching and research institutions in France or abroad, or from public or private research centers.

L'archive ouverte pluridisciplinaire **HAL**, est destinée au dépôt et à la diffusion de documents scientifiques de niveau recherche, publiés ou non, émanant des établissements d'enseignement et de recherche français ou étrangers, des laboratoires publics ou privés.



Distributed under a Creative Commons Attribution - NonCommercial 4.0 International License

Reaction pathways for the HDO of guaiacol over supported Pd catalysts: effect of support type in the deoxygenation of hydroxyl and methoxy groups

Camila A. Teles^{1,2}, Priscilla M. de Souza³, Raimundo C. Rabelo-Neto¹, Alejandra Teran⁴, Gary Jacobs^{4,5}, Clara Vilela⁶, Zuy M. Magriotis⁶, Vinicius O. O. Gonçalves⁷, Daniel. E. Resasco⁸, Fabio B. Noronha^{1,2,3*}

¹ National Institute of Technology, Catalysis Division, 20081-312, Rio de Janeiro, Brazil.

² Military Institute of Engineering, Chemical Engineering Department, 22290-270, Rio de Janeiro, Brazil.

³ Université of Lille, CNRS, Centrale Lille, ENSCL, Univ. Artois, UMR 8181 – UCCS – Unité de Catalyse et Chimie du Solide, F-59000 Lille, France

⁴ University of Texas at San Antonio, Department of Biomedical Engineering and Chemical Engineering, 1 UTSA Circle, San Antonio, TX 78249 USA.

⁵ University of Texas at San Antonio, Department of Mechanical Engineering, 1 UTSA Circle, San Antonio, TX 78249 USA.

⁶ Federal University of Lavras, Engineering Department, 37200-900, Lavras, Brazil

⁷ Federal University of Rio de Janeiro, Institute of Chemistry, Department of Physical Chemistry, 21949-900, Rio de Janeiro, Brazil.

⁸Center for Biomass refining, School of Chemical, Biological and Materials Engineering, The University of Oklahoma, Norman, OK, 73019, USA.

* Corresponding author: fabio.bellot@int.gov.br

Submitted to Journal of Molecular Catalysis A: Chemical

Revised January

2021

Abstract

The effect of support type (SiO_2 , CeO_2 , ZrO_2 , TiO_2 , Nb_2O_5) on the removal of the different oxygenated functional groups (hydroxyl and methoxy) was investigated in the hydrodeoxygenation (HDO) of guaiacol over Pd supported catalysts at 573 K and atmospheric pressure. The product distribution depended of the support type, and three main reaction pathways were proposed: demethoxylation, demethylation and dehydroxylation. Demethoxylation yielding phenol was the dominant reaction pathway over all catalysts with only a minor contribution from the demethylation reaction taking place. However, significant dehydroxylation reaction still observed for the catalysts having Pd supported on ZrO_2 , TiO_2 and Nb_2O_5 . Further conversion of phenol to cyclohexanone was favored over SiO_2 and CeO_2 -based catalysts, while benzene was only detected over ZrO_2 , TiO_2 and Nb_2O_5 , which is due to the presence of oxophilic cations. DRIFTS measurements were carried out to evaluate the adsorption mode and strength of guaiacol on the catalyst surface. The functional groups involved in adsorption of guaiacol included both hydroxyl and methoxy groups. At the reaction conditions, the hydroxyl group is strongly adsorbed to the catalyst surface and may block the catalytic sites, thus inhibiting further conversion of phenol and resulting in lower deoxygenation rates.

Keywords: Bio-oil; hydrodeoxygenation; guaiacol support effect.

1. Introduction

The bio-oil obtained from the pyrolysis process of lignocellulosic biomass is a promising resource towards the sustainable production of biofuels and chemicals in the face of increasing demand for energy coupled with a global concern to reduce CO₂ emissions. However, this liquid has poor quality in terms of energy content and stability due to the high content of oxygenated compounds within its composition. The catalytic hydrodeoxygenation (HDO) process is a promising approach to upgrade this bio-oil into valuable fuels, producing a liquid with high heating value and chemical stability [1-3].

The bio-oil is a complex mixture of several organic compounds that include simple oxygenates (acids, esters, alcohols, ketones, aldehydes), sugars, furans (e.g. furfural, hydroxymethyl furfural) and phenolic compounds (phenols, guaiacols, syringols) [4,5]. Such a complex composition makes it difficult to predict the HDO reaction mechanism, kinetics, active sites and structure-function relationships of the catalysts. As such, fundamental studies with model molecules that represent the families of compounds derived from biomass are being conducted.

Because functionalized phenols are major constituents in the bio-oil obtained from pyrolysis of the lignin fraction of biomass, compounds including phenol [6,7,8,9], cresols [10,11,12], anisole [13,14] and guaiacol [15,16] are the ones that are studied the most. These molecules contain hydroxyl and/or methoxy groups attached to the aromatic ring. The HDO of those molecules has been investigated over a variety of metal supported catalysts. It is widely accepted that bifunctional catalysts are required for the HDO reaction of phenolic compounds in which the hydrogenation reaction occurs over a metallic site and dehydration/deoxygenation takes place over the support [6,7,9,12-20]. From these studies, the type of metal and support plays an important role in the control of reaction pathways and deoxygenation activity.

Previous work by our group showed that the reaction pathways involved in the HDO of molecules containing a hydroxyl group, such as phenol and m-cresol, in the gas phase and at atmospheric pressure strongly depend on the type of metal and support [8,9,10,18,20-23]. For these types of molecules, a reaction mechanism based on enol/keto tautomerization was proposed. A keto tautomer intermediate is formed and may react by sequential hydrogenation of the aromatic ring to produce (methyl)-cyclohexanone and (methyl)-cyclohexanol, or by hydrogenation of the C=O bond producing an unsaturated alcohol which is rapidly dehydrated to benzene or toluene. These two different reaction routes depend on the type of catalysts. Metals such as Pt, Pd, Ni, Co supported on oxides such as SiO₂, CeO₂, Al₂O₃ promote the ring hydrogenation to produce the ketone and the alcohol, which can be dehydrated to (methyl)-cyclohexene in the presence of an acidic support. Oxophilic metals such as Ru or supports containing oxophilic sites such as ZrO₂, TiO₂ and Nb₂O₅ favor the selective hydrogenation of the carbonyl group or even the direct dehydroxylation to produce the deoxygenated product.

The HDO reaction mechanism for the removal of the methoxy group is widely investigated by testing anisole as a model molecule. In general, two reaction pathways may occur: (i) demethylation to produce a phenoxy species and its further hydrogenation to phenol or deoxygenation to benzene or (ii) direct demethoxylation toward benzene. As in the case of phenol and cresol, an important effect of metal type is observed with oxophilic metals such as Ru, Re, Fe, which promote the formation of benzene while less oxophilic metals such as Pt, Pd produce only hydrogenated products [24-28].

Guaiacol is a key molecule to simulate the bio-oil composition since its elemental composition is close to the overall elemental composition of lignin-derived

bio-oil in terms of H/O/C ratios [29]. Furthermore, guaiacol is useful for describing the reactivity and selectivity of catalysts towards conversion of both hydroxyl and methoxy groups attached to the aromatic ring. Consequently, a more complex reaction mechanism is expected with a variety of different reaction pathways involving hydrogenation, demethoxylation, demethylation, dehydroxylation, transalkylation and dehydration reactions depending on catalyst properties. For instance, the effect of metal type has been investigated [30]. However, there has not yet been a systematic study of the effect of support type in the HDO of guaiacol. In general, the few works discussing how the support type contributes to catalytic reactivity suggest that the acidity of supports likely affect the reaction pathways and product distributions [31,32]. However, most of these works were conducted in the liquid phase and at high H₂ pressure [15,33-36]. These factors make it difficult to directly comparison with our previous work using phenol and m-cresol in the gas phase. Concerning the proposed reaction pathways for HDO of guaiacol in the gas phase and at atmospheric pressure, the few works found in the literature report demethylation as the main reaction step [37-42]. Olcese et al. [29] tested an Fe/SiO₂ catalyst for the HDO reaction of guaiacol in the gas phase and obtained methane and phenol as main products followed by conversion of phenol towards benzene. A similar reaction pathway was proposed over nickel phosphide (Ni₂P) supported on various acidic substrates [37]. Similarly, Gonzalez-Borja et al. [26] observed higher yields of methane and benzene, which were produced from the conversion of phenol over Pt-Sn supported on carbon catalysts.

In the present work, guaiacol was used as a model molecule in order to investigate the effect of support type on the removal of both oxygenated functional groups (hydroxyl and methoxy) by gas phase reaction at atmospheric pressure. The investigation of catalytic performance in combination with DRIFTS measurements were

carried out over Pd supported on SiO₂, CeO₂, ZrO₂, TiO₂ and Nb₂O₅ catalysts to determine the reaction pathways.

2. Experimental section

2.1 Catalyst preparation

Tetragonal zirconia (ZrO₂) was supplied by Saint-Gobain NorPro. TiO₂ (Aeroxide TiO₂ P25) support was provided by Evonik Industries. SiO₂ (silica gel, Aldrich) was calcined under air flow (50 mL/min) using a heating rate of 5 K/min up to 1073 K, and then remaining at this temperature for 5 h. Nb₂O₅ support was obtained by calcination of niobic acid (CBMM) under air flow (50 mL/min) by heating at 5 K/min up to 673 K and then holding at this temperature for 4 h. CeO₂ was synthesized by the precipitation method. A solution of ammonium cerium (IV) nitrate ((NH₄)₂Ce(NO₃)₆, Sigma-Aldrich) was slowly added to a solution of 4.0 mol/L ammonium hydroxide (NH₄OH, Vetec) at room temperature and kept under vigorous stirring for 30 min. The resulting precipitate was filtered and washed with distilled water until a pH of 7 was reached. Then, the solids were dried at 383 K for 12 h and calcined under dry air flow at 773 K (heating ramp 5 K/min) for 6 h. The catalysts containing 2 wt. % Pd were prepared by incipient wetness impregnation of the supports with an aqueous solution of Pd(NO₃)₂ (solution of 20 wt% Pd in nitric acid, Umicore). After impregnation, each powder sample was dried in air at 393 K for 12 h and calcined at 673 K, 2 K/min for 3 h, under 50 mL/min of synthetic air flow.

2.2 Catalyst characterization

Surface areas were measured using a Micromeritics ASAP 2020 analyzer by nitrogen adsorption at the boiling temperature of liquid nitrogen. The total density of acid sites of the catalysts was investigated by temperature-programmed desorption of

ammonia (NH_3 -TPD). The samples (400 mg) were reduced at 573 K for 1 h under 60 mL/min of H_2 flow and then purged in He flow for 30 min. Then, the samples were cooled to 423 K and pure He flow was switched to a mixture containing 4% NH_3 in He (30 mL/min) for 30 min. The physisorbed ammonia was first flushed out with flowing He and then heated up to 773 K at 20 K/min under He flow. The dehydrogenation of cyclohexane was used as a structurally-insensitive reaction to estimate the metallic dispersion of the samples [9,18,23]. The fresh samples were first reduced at 573 K for 1 h and then cooled to the cyclohexane dehydrogenation reaction temperature (543 K). The reaction mixture was fed into the reactor after bubbling H_2 through a saturator containing cyclohexane kept at 285 K ($\text{H}_2/\text{C}_6\text{H}_{12} = 13.2$). The effluent was analyzed using an Agilent Technologies 7890A/5975C GCMS, equipped with an HP-Innowax capillary column and a flame-ionization detector (FID).

DRIFTS experiments of adsorbed guaiacol were carried out using a Nicolet iS-10 instrument with a DTGS-TEC detector and a Harrick Scientific praying mantis style reaction chamber with ZnSe windows. The samples (~ 100 mg) were first reduced under H_2 (60 mL/min) at 573 K, purged with He flow and then the temperature was decreased to 323 K in order to record a background spectrum. Helium was passed through a saturator containing guaiacol at 60 mL/min to carrier the vapor and the spectra were recorded. The saturator was kept at 360 K. After adsorption at 323 K, the temperature was increased at different temperatures under flowing He in order to desorb the organic molecule. Spectra were recorded at 323, 373, 473 and 573 K. Each spectrum was recorded with 512 scans at a resolution of 4 cm^{-1} .

2.3 Catalytic activity

The catalytic experiments were performed in a fixed-bed flow reactor in vapor-phase, operating at atmospheric pressure of H₂ and 573 K. Catalyst particles (53-106 μm) were diluted with SiC particles (200-450 μm, m_{SiC}/m_{catalyst} = 3.0) in order to avoid localized overheating. Prior to reaction, the catalysts were reduced *in situ* under pure hydrogen (60 mL/min) at 573 (10 K/min) for 1 h. The reactant mixture was obtained by flowing H₂ through the saturator containing guaiacol, which was kept at 359 K to obtain the desired H₂/guaiacol molar ratio of 60. To avoid condensation, all lines were heated to 523 K.

The catalysts were tested at different W/F ratios, by varying catalyst amount in order to obtain low conversion. W/F is defined as catalyst mass (W, g) divided by mass flow rate (F, g/h) of the organic feed. Initial conversion was measured after 5 min of reaction to minimize the effect of catalyst deactivation. The reaction products were analyzed using an Agilent Technologies 7890A/5975C GCMS, equipped with an HP-Innowax capillary column and a flame-ionization detector (FID).

The conversion, product selectivity and HDO reaction rate were calculated as follows:

$$Conversion(\%) = \frac{mol_{feed}^0 - mol_{feed}}{mol_{feed}^0} \times 100 \quad (1)$$

$$Selectivity(\%) = \frac{mol_i}{mol_{feed}^0 - mol_{feed}} \times 100 \quad (2)$$

$$Rate_{HDO}(mmol g^{-1}_{cat} \text{ min}^{-1}) = \frac{yield \text{ of deoxygenated product} * F}{W} \quad (3)$$

where $\text{mol}_{\text{feed}}^0$ and mol_{feed} are the number of moles of the organic feed initial and after reaction, mol_i is the number of mols of a given i product.

3. Results and Discussion

3.1. Catalyst Characterization

The specific areas of the catalysts are reported in Table 1. The Pd/SiO₂ catalyst showed the highest surface area (153 m²/g), while the lowest values were observed for Pd/CeO₂ and Pd/TiO₂, 56 and 54 m²/g, respectively.

The Pd dispersion for the different catalysts was estimated by using cyclohexane dehydrogenation as a probe reaction (Table 1). Pd/ZrO₂ and Pd/TiO₂ exhibited the highest metallic dispersion (70 and 63% respectively), whereas Pd/CeO₂ and Pd/Nb₂O₅ showed Pd dispersions around 27 and 22%, respectively. The lowest Pd dispersion was observed for the Pd/SiO₂ catalyst (13%).

In order to measure the density of the acid sites, NH₃-TPD was carried out. The amount of ammonia desorbed is listed in Table 1. The amount of ammonia desorbed from Pd/SiO₂ was negligible. Pd/ZrO₂ exhibited the highest specific number of acid sites, which is likely due to the well-known acidity reported for tetragonal zirconia [21]. The following order was observed for the number of acid sites: Pd/ZrO₂ > Pd/Nb₂O₅ > Pd/TiO₂ >> Pd/CeO₂ >> Pd/SiO₂.

3.2 HDO of guaiacol

Figure S1 shows the guaiacol conversion and product yield as a function of W/F for HDO of guaiacol at 573 K. Regarding product distribution, phenol, benzene, methanol, methane and anisole are the main products obtained, while cyclohexanone, cyclohexane and methoxy-cyclohexane are minor products. For all catalysts, phenol and methanol are mainly produced over the entire range of W/F, indicating that the demethoxylation is the main reaction pathway. For Pd/Nb₂O₅, Pd/ZrO₂, Pd/TiO₂ catalysts, significant formation of methane and benzene is also observed, whereas

benzene was not detected even at higher values of guaiacol conversion for the Pd/SiO₂ catalyst.

The HDO reaction rate and the product distribution obtained at low conversion of guaiacol are listed in Table 2. Among the catalysts, Pd/TiO₂ and Pd/Nb₂O₅ were the most active catalysts for HDO, while Pd/SiO₂ and Pd/CeO₂ catalysts exhibited almost negligible activity. The rate of deoxygenation followed the order: Pd/TiO₂ (0.063) > Pd/Nb₂O₅ (0.047) > Pd/ZrO₂ (0.022) > Pd/CeO₂ (0.003) ≈ Pd/SiO₂ (0.00). No relationship is observed between the HDO reaction rate and metal dispersion (Table 1), suggesting that the deoxygenation rate is not only dependent on metal dispersion. This was also previously reported by de Souza et al. [21,43] for the HDO of phenol and m-cresol over Pd/ZrO₂ catalysts. Pd/ZrO₂ catalysts with different Pd dispersions exhibited approximately the same TOF for deoxygenation of phenol and m-cresol. Likewise, there is no correlation between the activity for HDO of guaiacol and catalyst acidity. The variation in the density of acid sites (Pd/ZrO₂ > Pd/Nb₂O₅ > Pd/TiO₂ >> Pd/CeO₂ >> Pd/SiO₂) does not correspond to that observed for the guaiacol deoxygenation rate (Pd/TiO₂ > Pd/Nb₂O₅ > Pd/ZrO₂ >> Pd/CeO₂ ≈ Pd/SiO₂). Boonyasuwat et al. [44] investigated the performance of Ru supported on SiO₂, C, Al₂O₃ and TiO₂ catalysts for the HDO of guaiacol in the gas phase. Ru/Al₂O₃ catalyst exhibited higher acidity but lower activity compared to Ru/TiO₂ and even Ru/C catalysts. Barrios et al. [18] and Teles et al. [23] tested a series of different catalysts with a wide range of acidity for the HDO of phenol in the gas phase at similar reaction conditions and no correlation was also observed between the density of acid sites and deoxygenation activity. In general, the catalyst acidity plays an important role for the HDO reaction conducted in the liquid phase and at high hydrogen pressure, where saturation of the ring initially occurs to

form the respective alcohol with further dehydration to the deoxygenated product over acid sites [45-48].

The Pd-based catalysts investigated on HDO of guaiacol in this work were also previously tested for the HDO of phenol, m-cresol and anisole. The rate of guaiacol deoxygenation was lower in comparison to the deoxygenation rate of other phenolic compounds for the same catalysts and tested under similar reaction conditions [9,21]. Fig. 1 shows a comparison between the HDO of guaiacol reaction rate obtained in this work with the rate for HDO of phenol and anisole over the same catalysts, previously investigated by Teles et al. [49]. The deoxygenation rate of phenol is significantly higher compared to anisole, indicating that the removal of the hydroxyl group is more facile compared to the removal of the methoxy group at these reaction conditions. The HDO rate of guaiacol is still lower compared to anisole, which may be due to a steric hindrance effect in this compound caused by the methoxy group being adjacent to the hydroxyl group [50,51]. Foo et al. [41] compared the performance of Pt/HBeta catalysts for the HDO of m-cresol, anisole and guaiacol molecules at 400 °C and 1 atm. Similarly, the authors found a lower activity for the HDO of guaiacol. By comparison of catalytic results and *in situ* FTIR spectroscopy analysis during the reactions, they suggested that steric hindrance plays an important role in the degree of deoxygenation, especially with an adjacent functional group as is the case of guaiacol. Based on DFT calculations, Dwiatmoko et al. [52] observed that the adsorption energy of guaiacol on a Ru surface (1.33 eV) is lower in comparison to benzene (1.41 eV) considering a flat adsorption, which is due to the presence of a methoxy and hydroxyl group that induces a steric effect, weakening the binding between the model compound and the catalyst surface.

However, significant differences are observed depending on the type of support. Phenol is mainly produced on Pd/SiO₂ and Pd/CeO₂ catalysts. In addition, CH₄ is formed to a minor extent, suggesting that demethylation occurs to produce catechol as the intermediate. However, catechol was not observed as a reaction product due to its rapid dehydration to phenol or because it may remain adsorbed on the catalyst surface. Other works in the literature also reported that catechol could not be detected even at short contact times [26,38,42,53]. The C₁/C₆ ratio (C₁: methane and methanol; C₆: phenol, benzene, cyclohexanone, cyclohexanol, cyclohexane) was calculated in order to assure that catechol was completely converted to phenol. For all catalysts, this ratio was close to 1.0, indicating that all catechol initially formed rapidly converted to phenol, which in turn reacted to benzene or cyclohexanone and cyclohexanol. The Pd/ZrO₂ catalyst exhibited the highest selectivity to CH₄. Benzene was mainly produced over Pd/Nb₂O₅, Pd/ZrO₂, Pd/TiO₂, whereas it was not detected on Pd/CeO₂ and Pd/SiO₂. In this case, benzene could be produced from the deoxygenation of phenol or even from anisole. In general, the selectivity towards deoxygenation products (benzene and cyclohexane) followed the order: Pd/Nb₂O₅ (15.7%) \approx Pd/ ZrO₂ (15.0%) > Pd/TiO₂ (13.4%) \gg Pd/CeO₂ (0.4%) \approx Pd/SiO₂ (0.0 %).

Minor products, such as a methoxy-cyclohexanone, were formed from the selective hydrogenation of the aromatic ring of guaiacol and these products were mainly produced on the Pd/CeO₂ catalyst. The carbonyl group of this compound can be hydrogenated to the alcohol and dehydrated over the acid sites of Pd/ZrO₂, Pd/TiO₂ and Pd/Nb₂O₅ catalysts to produce methoxy-cyclohexene and subsequently hydrogenated to methoxy-cyclohexane. However, only traces of this compound were observed. Products such as o-cresol, m-cresol and biphenyl are formed in traces by transalkylation and

alkylation reactions via the acid sites of Pd/ZrO₂, Pd/TiO₂ and Pd/Nb₂O₅ catalysts

[54,55]

3.3 DRIFTS of the adsorbed molecules

In order to understand the reaction pathways observed in the HDO of guaiacol, as well as to investigate the mode and strength of adsorption of the guaiacol molecule on the catalyst surface, DRIFTS spectra were recorded during a TPD experiment after adsorption of guaiacol. The catalysts were exposed to a guaiacol/He mixture and TPD was carried out under 60 mL/min of He flow at different temperatures (323-573 K). Three catalysts were chosen to perform the DRIFTS experiments: the less oxophilic Pd/CeO₂ and the two more oxophilic and active catalysts (Pd/TiO₂ and Pd/Nb₂O₅). The assignments of the vibrational wavenumbers observed in the spectra were performed by comparison with previous spectroscopic studies of adsorbed phenolic compounds found in the literature [9, 56-63], as shown in Table 3.

Figs. 2-4 shows the DRIFTS spectra of adsorbed guaiacol over the different catalysts. The spectra consist of three sets of bands: (i) $\nu(\text{C-H})$ stretching mode in the region between 3100 to 2770 cm⁻¹; (ii) $\nu(\text{C=C})$ stretching mode characteristic of the aromatic ring in the region between 1600 to 1490 cm⁻¹ and (iii) $\nu(\text{C-O})$ stretching mode in the region below 1300 cm⁻¹. The guaiacol molecule contains a methoxy group attached to the aromatic ring, and therefore, it is expected to present two sets of C-H stretching bands corresponding to (1) the C_{sp2}-H bond of the aromatic ring and (2) the C_{sp3}-H from the methoxy group. In addition, one band in the region of 1454-1460 cm⁻¹ attributed to the $\delta(\text{CH}_3)$ vibration of the methyl group should be observed. Similarly, at least three bands characteristic of C-O bond (C_{Ar}-OH, C_{Ar}-OCH₃, H₃C-O) are expected.

In this work, at the first desorption temperature (323 K), similar bands were observed for all catalysts. For the Pd/CeO₂ catalyst, the spectrum shows bands positioned at 3063, 2942, 2836 cm⁻¹, which are characteristic of $\nu(\text{C-H})$ stretching mode; bands located at 1594 and 1495 cm⁻¹ corresponding to the $\nu(\text{C=C}_{\text{ring}})$ stretching

mode of the aromatic ring; a band at 1455 cm^{-1} attributed to the asymmetrical $\delta(\text{CH}_3)$ vibration of the methoxy group and bands at 1293 , 1254 , 1213 and 1115 cm^{-1} that should be assigned to the $\nu(\text{C-O})$ vibrational modes. For the Pd/TiO₂ and Pd/Nb₂O₅ catalysts, similar bands are observed. However, the relative intensities of the bands at $1584 - 1589\text{ cm}^{-1}$ and $1499 - 1497\text{ cm}^{-1}$, assigned to the $\nu(\text{C}=\text{C}_{\text{ring}})$ stretching mode of the aromatic ring, were lower compared to those observed for the Pd/CeO₂ catalyst.

According to the vibrational mode assignment of the bands for the adsorbed phenolics compounds found in the literature (Table 3), the characteristics bands of $\nu(\text{C}_{\text{Ar}}\text{-OH})$ and $\nu(\text{C}_{\text{Ar}}\text{-OCH}_3)$ appear in the region between $1225\text{-}1295\text{ cm}^{-1}$ while the band of $\nu(\text{H}_3\text{C-O})$ should appear in the region between $1000\text{-}1114\text{ cm}^{-1}$. Depending on the nature of the oxide support, the bands related to C_{Ar}-OH and C-OCH₃ may appear as one or two bands.

According to Popov et al. [59,60] and Mariey et al. [64], the adsorption of phenol on an oxide surface exhibits a DRIFTS spectrum with the band associated with the $\nu(\text{C}_{\text{Ar}}\text{-OH})$ splitted into two components that correspond to the formation of two phenolates, mono and bidentate that appear at around 1250 and 1295 cm^{-1} . Teles [50] performed similar experiments of DRIFTS adsorption of phenol on Pd/CeO₂, Pd/TiO₂ and Pd/Nb₂O₅ catalysts. The spectrum of adsorbed phenol on the Pd/CeO₂ surface showed a broad band at 1275 cm^{-1} associated with the phenoxy species. However, the spectra of Pd/TiO₂ and Pd/Nb₂O₅ catalysts showed a doublet at around 1286 and 1260 cm^{-1} suggesting the presence of a mono and bidentate phenoxy species, as suggested by Popov et al. [60,61] and Mariey et al. [64].

For the spectra of adsorbed anisole, Mathew et al. [58] and Popov et al. [60] observed a band at 1245 cm^{-1} that was attributed to C_{Ar}-OCH₃ bond of adsorbed methoxy species, while the band at 1290 cm^{-1} was assigned to C_{Ar}-O* bond of the

phenoxy species formed by dissociative adsorption of anisole. Teles [49] also observed two intense bands at 1296 and 1245 cm^{-1} on the spectra of adsorbed anisole on Pd/CeO₂ catalyst, which were attributed to the C_{Ar}-O* and C_{Ar}-OCH₃ bond vibrations, respectively. There was also a band at 1035 cm^{-1} corresponding to the H₃C-O bond. For the Pd/TiO₂ and Pd/Nb₂O₅ catalysts, only one band was detected at around 1245 cm^{-1} relative to the C_{Ar}-OCH₃ bond while the band associated with the H₃C-O bond was observed at 1114 cm^{-1} .

Based on the spectra obtained for these two individual molecules (Table 3), our spectra of adsorbed guaiacol suggests the presence of both phenoxy and methoxy groups adsorbed on the catalyst surface. Therefore, the bands located at 1594-1484 and 1499 - 1495 cm^{-1} corresponds to the $\nu(\text{C}=\text{C}_{\text{ring}})$ stretching mode of the aromatic ring; the band at 1455 cm^{-1} is attributed to the asymmetrical $\delta(\text{CH}_3)$ vibration of the methoxy group; the bands at around 1290 and 1250 cm^{-1} are likely associated with the adsorption of phenoxy species (monodentate and bidentate), formed by the dissociative adsorption of guaiacol. The band at 1250 cm^{-1} can also be related to the adsorption of guaiacol by the methoxy group. Another band is observed between 1213 and 1224 cm^{-1} that it is not observed in the spectra of pure adsorbed phenol or anisole. Popov et al. [59] found this band in the spectrum of adsorbed guaiacol on Al₂O₃ that was attributed to the vibration of C_{Ar}-OCH₃ bond. Finally, the band at 1115 cm^{-1} is due to the vibration of the H₃C-O bond [65]. Then, it is hard to distinguish the mode of adsorption of guaiacol molecule on the catalyst surface by the $\nu(\text{C}-\text{O})$ stretching mode in the region between 1300 - 1200 cm^{-1} due to the overlapping contributions of hydroxyl and methoxy groups. However, the bands observed for the $\delta(\text{CH}_3)$ and H₃C-O bond vibration give evidences of adsorption of the methoxy group. Thus, the adsorption of the guaiacol molecule on the catalyst surface through doubly anchored species (hydroxyl and methoxy groups) and

the formation of strongly bound species (bidentate surface species) might block some of the active sites inhibiting further steps in the reaction mechanism. This result agrees with the lower HDO reaction rates of guaiacol in comparison to the HDO of phenol or anisole.

Increasing the temperature to 373 K, the spectra for all catalysts remained unchanged. However, raising the temperature to 473 K caused a small decrease in the intensities of all bands. At our reaction temperature (573 K), the intensity of the bands significantly decreased, especially for the Pd/TiO₂ and Pd/Nb₂O₅ catalysts. Furthermore, the intensities of the bands at 1455 cm⁻¹ attributed to the $\delta(\text{CH}_3)$ vibration mode and at 1115 cm⁻¹ attributed to the $\nu(\text{C-O})$ vibration mode of the H₃C-O bond of the methoxy group strongly decreased and a slight shift to lower wavenumbers was even observed, while the bands related to the $\nu(\text{C}=\text{C}_{\text{ring}})$ stretching mode of the aromatic ring and the bands associated with the phenoxy species (around 1250 cm⁻¹) remain intense. This suggests that at our reaction temperature, there is the cleavage of the C_{Ar}-OCH₃ bond from methoxy group producing methanol and thus the phenoxy species remains more strongly adsorbed on the catalyst surface.

3.4 Proposed reaction pathways for the HDO of guaiacol

In this work, we investigated the HDO reaction of guaiacol over different supported Pd catalysts to study the effect of support type on the deoxygenation of this molecule. The HDO of guaiacol may occur through hydrogenolysis of the C_{Ar}-O from hydroxyl or methoxy groups [29]. However, because of the high energy barrier associated with the cleavage of C_{Ar}-O bonds, alternative routes are proposed in the literature. The three types of C-O bond in guaiacol molecule have different C-O dissociation energies: (i) C_{Ar}-OH: 414 kJ/mol; (ii) C_{Ar}-OCH₃: 356 kJ/mol; (iii) C_{Ar}O-

CH₃: 217 kJ/mol [66]. Thus, demethylation with the production of catechol as a reaction intermediate should be the most facile reaction. Once formed, catechol is further deoxygenated to phenol. In the present work, methane is formed but catechol is not observed, suggesting that catechol may be rapidly converted to phenol or it may remain adsorbed on the catalyst surface. In contrast to demethylation, demethoxylation via C_{Ar}-OCH₃ bond cleavage producing phenol should be less favorable. However, in this work, phenol and methanol were the main products formed approximately with the same selectivity, indicating that phenol is directly produced through the cleavage of the C_{Ar}-OCH₃ bond for all catalysts. Curiously, this is the main reaction pathway even for the Pd/SiO₂ and Pd/CeO₂ catalysts that show low activity for the deoxygenation of other phenolic compounds such as phenol [9,23].

Phenol can be further converted to benzene, cyclohexanone and cyclohexanol via the tautomerization mechanism previously proposed for the HDO reaction of phenol using similar catalysts and reaction conditions [9,18,21]. By the tautomerization mechanism, an unstable keto intermediate is formed and may react by two different reaction pathways. The first one involves the hydrogenation of the aromatic ring producing cyclohexanone, which is also hydrogenated to cyclohexanol. The alcohol can be further dehydrated to cyclohexene in the presence of a catalyst with enough acidity. In our case, the hydrogenation route was promoted by the Pd/SiO₂ and Pd/CeO₂ catalysts. In the second reaction pathway, the carbonyl group is preferentially hydrogenated leading to the formation of an unsaturated alcohol, which is rapidly dehydrated to benzene. This route was favored by the Pd/ZrO₂, Pd/TiO₂ and Pd/Nb₂O₅ catalysts due to the presence of oxophilic sites. De Souza et al. [9] and Barrios et al. [18] found the following order for the selectivity towards benzene from HDO of phenol: Pd/Nb₂O₅ (83%) > Pd/TiO₂ (67%) > Pd/ZrO₂ (44%) > Pd/CeO₂ (4%) ≈ Pd/SiO₂ (3%).

The results obtained in this work agree very well with the results obtained for the HDO of phenol. Pd/SiO₂ and Pd/CeO₂ catalysts favored the formation of hydrogenated products while Pd/ZrO₂, Pd/TiO₂ and Pd/Nb₂O₅ catalysts promoted the formation of benzene. However, lower selectivity to benzene is achieved for the HDO of guaiacol (around 15 % for these three catalysts) in comparison to the results obtained for HDO of phenol and m-cresol. This may be due to the steric hindrance effects on this molecule and the blocking of the active sites by the strong adsorption of guaiacol hampering secondary reactions. Furthermore, similar selectivity to benzene was obtained for these three catalysts, contrary to the larger difference reported for the HDO of phenol directly.

Anisole is produced by the dehydroxylation of guaiacol. Since the cleavage of the C_{Ar}-OH bond requires higher energy compared to the cleavage of the C_{Ar}-OCH₃ bond (414 and 356 KJ/mol respectively) [66], the production of phenol by demethoxylation rather than dehydroxylation is expected to occur. This is in agreement with our higher selectivity to phenol, implying that the removal of the methoxy group is more favorable than deoxygenation by removal of hydroxyl group. In this work, the highest selectivity to anisole was obtained for Pd/ZrO₂, Pd/TiO₂ and Pd/Nb₂O₅ catalysts due to the presence of oxophilic sites. Once formed, anisole can be further converted to benzene or phenol by the reaction pathways proposed in the literature for the HDO of anisole in the gas phase. According to Tan et al. [25] anisole can react via three main reaction pathways: (i) ring hydrogenation producing methoxycyclohexane; (ii) demethoxylation to produce benzene; (iii) demethylation to produce a phenoxy intermediate species, which can be hydrogenated to phenol or the cleavage of the C-O* may occur, producing benzene. Once phenol is produced, further reaction cannot be excluded via the previously proposed tautomerization mechanism. Tan et al. [25] tested a series of Pt, Ru and Fe supported on silica catalysts for the HDO of anisole in the gas phase and

compared with DFT calculations. The authors proposed demethylation as the main reaction pathway producing the phenoxy intermediate. Oxophilic metals such as Ru and Fe promote the cleavage of the C-O* bond to produce benzene while less oxophilic metals favored the hydrogenation of the intermediate yielding phenol. However, Teles et al. [49] tested Pd supported on SiO₂ and Nb₂O₅ catalysts under similar reaction conditions and observed demethylation as the main reaction pathway for Pd/SiO₂. However, direct demethoxylation was favored over the Pd/Nb₂O₅ catalyst, which was explained by the presence of Nb⁵⁺/Nb⁴⁺ oxophilic cations. Based on these observations, the main reaction pathways for the HDO of guaiacol, considering the product distribution obtained in this work, may be summarized as shown in Scheme 1.

There are few works in the literature investigating the HDO reaction of guaiacol in the gas phase at atmospheric pressure [26,29,37-42]. Researchers have examined several catalysts for this reaction; however, a systematic study of the effect of the support type on the reaction mechanism is missing. For instance, Wu et al. [67] reported the conversion of guaiacol over Ni₂P supported on SiO₂, Al₂O₃ and ZrO₂ catalysts. The same reaction pathways were proposed in that work, with Ni₂P/SiO₂ catalyst promoting demethoxylation and yielding phenol, followed by deoxygenation to benzene. Ni₂P/Al₂O₃ and Ni₂P/ZrO₂ catalysts promoted the demethylation route, producing catechol as the main reaction product. The enhanced deoxygenation activity of Ni₂P/SiO₂ was attributed to the morphology of the phosphate phase, with more P-OH species for hydrogen transfer. Oyama's group [37] also investigated supported Ni phosphide catalysts, in this case using acid supports such as SiO₂-Al₂O₃, ZSM5 and USY zeolites. Demethylation was the main reaction pathway proposed and a correlation was proposed between the number of Lewis acid of the catalysts (Ni₂P/SiO₂-Al₂O₃ > Ni₂P/ZSM5 > Ni₂P/USY) and the formation of catechol. The conversion of guaiacol in

the gas phase was also performed by Boonyasuwat et al. [44] over a series of Ru supported catalysts (Ru/C, Ru/SiO₂, Ru/Al₂O₃, Ru/TiO₂). They also reported an important role of the support type on the deoxygenation activity. The selectivity toward the deoxygenated product followed the order: Ru/TiO₂ > Ru/SiO₂ > Ru/C > Ru/Al₂O₃. The highest activity of Ru/TiO₂ catalyst was attributed to the creation of defect sites on TiO₂ by the Ru metal particles that may affect the adsorption of guaiacol and the intermediate catechol on the catalyst surface. Theoretical studies regarding the interaction of catechol and anatase TiO₂ with and without defects were performed by Xu et al. [68]. Dissociative adsorption on a defect site was found to be stronger (274 kJ/mol) than on defect-free TiO₂ (78 kJ/mol). These results were confirmed by tests carried out with catechol over the Ru/TiO₂ catalyst, and a very fast conversion towards phenol was observed.

Although an important effect of the support is observed in those works, the effect of the support properties such as acidity or oxophilicity in the deoxygenation activity of guaiacol has not been explored to a significant extent. Evidence of the influence of catalyst oxophilicity was reported by Fang et al. [69], when Ni-Fe bimetallic catalysts were tested for the HDO of guaiacol in the gas phase. The product distribution was found to be dependent on the Ni/Fe atomic ratio due to the combination of the high capacity of Ni to activate H₂ and the strong oxophilicity of Fe to promote the oxygen activation and thus deoxygenation. Liu et al. [70] suggested that the cleavage of the three different C-O bonds present in the guaiacol molecule on NiFe(111) and PtFe(111) are energetically more favorable compared with the monometallic Ni(111) and Pt(111) planes. Recently, Zhou et al. [71] performed an interesting DFT study for the HDO of catechol on Ni(111) surface, Fe@Ni(111) single-atom alloy and NiFe(111) homogeneous alloy. It was shown that the deoxygenation performance is greatly

enhanced by alloying with oxophilic Fe. DFT calculations showed that the catechol adsorbed on Fe@Ni(111) and NiFe(111) has a C-OH bond more elongated than on Ni(111) surface and that OH groups prefer the direct interaction with the oxophilic Fe in comparison with Ni, resulting in the activation of C-O bonds.

Therefore, the oxophilicity is a key factor in the deoxygenation of guaiacol and this work underscores the effect of the oxophilic sites on the support and its combination with a metal in the control of the different reaction pathways involved for HDO of guaiacol.

3.5 Hydrodeoxygenation of the different bio-oil model molecules

The HDO reaction of phenolic model compounds such as phenol and anisole over Pd/SiO₂, Pd/CeO₂, Pd/ZrO₂, Pd/TiO₂ and Pd/Nb₂O₅ catalysts was previously investigated by Teles et al. [18,22,23,49]. In the present work, the same catalysts were tested for the HDO of guaiacol at the same reaction conditions. In this way, the effect of the type of support can be correlated with the reactivity of the different functional groups and their position in the aromatic ring.

According to Teles et al. [18,22,23,49], the HDO of phenol over the Pd/SiO₂ and Pd/CeO₂ catalysts produced mainly hydrogenated products (cyclohexanone, cyclohexanol). For the HDO of anisole, phenol, methane and methoxycyclohexane were the main products formed, indicating that the cleavage of the C_{alkyl}-O bond yielding a phenoxy intermediate is the main reaction pathway. However, further deoxygenation toward benzene through the cleavage of the C_{Ar}-O bond does not occur over these catalysts. For the HDO of guaiacol, the main reaction pathway is the demethoxylation producing phenol and methanol as major products. However, no evidence of further

deoxygenation to benzene is observed, since the deoxygenation of phenol (formed after demethoxylation) is more difficult over these catalysts.

The conversion of phenol for the Pd/ZrO₂, Pd/TiO₂ and Pd/Nb₂O₅ catalysts produced mainly deoxygenated products (benzene), in agreement with reports in the literature, which revealed higher deoxygenation activity for these supports [7,9,12,18]. For the HDO of anisole over Pd/ZrO₂ and Pd/TiO₂ catalysts, the results revealed the cleavage of the C_{alkyl}-O bond from the methoxy group producing a phenoxy intermediate as the major reaction pathway, in which benzene is further produced via tautomerization of phenol (formed via hydrogenation of the phenoxy intermediate) or via direct C-O* scission. Interestingly, for the Pd/Nb₂O₅ catalyst, the direct demethoxylation was the main reaction pathway. For the HDO of guaiacol, the formation of the final deoxygenated product (benzene) was only observed for Pd/ZrO₂, Pd/TiO₂ and Pd/Nb₂O₅ catalysts. Therefore, the HDO of phenolic compounds strongly depended on the type of support but this raises the question: what property of the support is required to enhance the HDO activity?

There are different proposals in the literature concerning the active site for the HDO reaction. There is generally a consensus that the HDO reaction requires a bifunctional catalyst: a metal associated with a specific support. Some studies suggest that the reaction takes place on the metal sites close to an acid site. Other works propose that the oxophilicity or the oxygen vacancies are the fundamental properties of the support to promote the deoxygenation. In our previous studies [8,9,18,19,22,23] as well in the present study, we have shown that HDO in the gas phase does not depend on catalyst acidity, regardless of the nature of the phenolic compound (phenol, m-cresol, anisole, guaiacol).

The effect of oxygen vacancies has also been considered to favor the deoxygenation of phenolic compounds. Chen and Pacchioni [72] suggested that the oxygen vacancies at the Ru-TiO₂ interface adsorb the O atom of phenol, promoting the cleavage of C-O bond. It is known that metal supported on reducible metal oxides such as TiO₂ or CeO₂ can partially reduce the support and lead to different degree of metal-support interaction (SMSI effect) [73]. However, the SMSI effect is usually observed after reduction of the catalyst at high temperature such as 773 K [74]. Zhao et al. [75] investigated the influence of SMSI effect on the performance of Pt/TiO₂ catalyst for HDO of m-cresol at 623 K by varying reduction temperatures from 623 K to 823 K. The characterization results (H₂-TPR, TEM, CO chemisorption, XPS) showed evidences of different degrees of metal-support interaction depending on the reduction temperature, which was attributed to the partial coverage of Pt surface by reduced TiO_x species with a varied extent. The TOF of toluene formation increased by 3 times when the reduction temperature increased from 623 to 823 K. Newman et al. [7] also reported an improved selectivity toward direct deoxygenation of phenol over a Ru/TiO₂ catalyst and attributed it to the formation of reduced titania sites created by hydrogen spillover, which strongly interacts with the phenol hydroxy group. Similar results were observed by Boonyasuwat et al. [44] for the HDO of guaiacol over a Ru/TiO₂ catalyst. However, in both studies, the catalysts were reduced at 673 K. Our group previously investigated the effect of oxygen vacancies (Pd/Ce_xZr_{1-x}O₂) [23] and the effect of partially coverage of metal surface by the reduced support (Pd/Nb₂O₅) [18] for the HDO of phenol at 573 K. The density of oxygen vacancies increased by introducing zirconium cations in the lattice of CeO₂ but no correlation was observed with the deoxygenation activity for phenol. However, the HDO activity increased due to the exposure to a higher density of the oxophilic Zr⁴⁺/Zr³⁺ cations. Pd/Nb₂O₅ catalyst was tested for HDO of phenol after

reduction at 573 or 773 K. The reaction rate decreased due to the coverage of Pd particles by partially reduced NbO_x species formed. However, the product distribution remained unchanged, suggesting that the defect sites created during reduction do not play an important role in the selectivity to the deoxygenated products.

In fact, the presence of an oxophilic site that strongly interacts with the oxygen atom of the model molecule, promotes the selective C=O bond hydrogenation or C-O bond cleavage. The strength of the interaction between the oxygen atom from a carbonyl group and the cation of the support for the different supported Pd catalysts was measured by DRIFTS experiments of adsorbed cyclohexanone and the results are plotted in Fig. 5a [9,18,23]. Pd/Nb₂O₅ exhibited the highest oxophilicity among the catalysts.

The catalyst deoxygenation ability for all model molecules was expressed by a deoxygenation/hydrogenation ratio. For the HDO of phenol (Fig. 5b), the trend of support oxophilicity agrees very well with the deoxygenation capacity exhibited by the catalysts, indicating that deoxygenation of the hydroxyl group strongly depends on the support oxophilicity. The same result is basically observed for the HDO of anisole and guaiacol (Figs. 5c and d). In addition, a very oxophilic support such as niobia can directly break the C_{Ar}-OCH₃ bond, producing benzene with higher values of HDO rates. The variation of deoxygenation/hydrogenation ratio for the HDO of guaiacol is similar to the trend for phenol, confirming that once guaiacol is converted to phenol, it is further transformed by the same reaction mechanism. However, the HDO reaction rate for guaiacol is very low as compared to the other molecules (Fig. 1) due to steric hindrance effects. Therefore, the results obtained in our work revealed that support oxophilicity plays a key role in the deoxygenation of phenolic molecules representative

of the lignin fraction, which may contribute to the design of more efficient catalysts for HDO of bio-oil.

4. Conclusions

In this work, the effect of the type of support was investigated for the HDO reaction of guaiacol in the gas phase at atmospheric pressure. Based on the catalytic results and depending on the type of support, three main reaction pathways were proposed: (i) demethoxylation to produce phenol, which is further converted to benzene or cyclohexanone and cyclohexanol; (ii) demethylation producing catechol as intermediate that is dehydrated to phenol and (iii) dehydroxylation to produce anisole, which can be also further converted to benzene or phenol. Demethoxylation was the dominant reaction pathway regardless of the type of support. However, additional conversion of phenol is favored by the more oxophilic catalysts Pd/ZrO₂, Pd/TiO₂ and Pd/Nb₂O₅ as well as the dehydroxylation reaction to produce anisole. In general, the deoxygenation of guaiacol molecule proceeds through the same reaction pathways observed for HDO of phenol and anisole, in which the formation of deoxygenated products is strongly dependent on catalyst oxophilicity. DRIFTS experiments revealed that the guaiacol molecule adsorbs simultaneously via hydroxyl and methoxy groups. At our reaction temperature, the hydroxyl group is still strongly adsorbed onto the catalyst surface, blocking the active sites and impeding the HDO of guaiacol reaction rate. In general, the results showed that the removal of the methoxy group occurs more easily while the removal of hydroxyl group is strongly dependent on catalyst oxophilicity, as previously shown for the HDO of phenol and m-cresol.

Acknowledgments

The authors thank Coordenação de Aperfeiçoamento de Pessoal de Ensino Superior (CAPES - Finance code 001), CAPES – COFECUB program (88881.142911/2017-01), Fundação de Amparo à Pesquisa do Estado do Rio de Janeiro (FAPERJ – E-26/202.783/2017) and Conselho Nacional de Desenvolvimento Científico e Tecnológico (CNPq - 303667/2018-4; 305046/2015-2; 302469/2020-6) for scholarship and financial support. This study was also supported by the French government through the Programme Investissement d’Avenir (I-SITE ULNE / ANR-16-IDEX-0004 ULNE) managed by the Agence Nationale de la Recherche, CNRS, Métropole Européen de Lille (MEL) and Region Hauts-de-France for “CatBioInnov” project are also acknowledged. Research conducted at UTSA was supported by UTSA, the State of Texas, and the STARS program. Alejandra Teran would like to thank the UTSA Office of Undergraduate Research, as well as the College of Engineering, for financial support through undergraduate research grants.

References

- [1] M.I. Jhirul, M.G. Rasul, A.A. Chowdhury, N. Aswath, *Energies* 5 (2012) 4952-5001.
- [2] N. Yan, Y. Yuan, R. Dykeman, Y. Kou, P.J. Dyson, *Anew. Chem. Int. Ed.* 49 (2010) 5549-5553.
- [3] Y. Elkasabi, C.A. Mullen, A.L. Pighinelli, A.A. Boateng, *Fuel Process Technol.* 123 (2014) 11-18.
- [4] H. Wang, J. Male, Y. Wang, *ACS Catal.* 3 (2013) 1047-1070.
- [5] M. Patel, A. Kumar, *Renew. Sust. Energ. Rev.* 58 (2016) 1293-1307.
- [6] A.J.R. Hensley, Y. Wang, J-S. McEwen, *ACS Catal.* 5 (2015) 523-536.

- [7] C. Newman, X. Zhou, B. Goundie, I.T. Ghampson, R.A. Pollock, Z. Ross, M.C. Wheeler, R.W. Meulenberg, R.N. Austin, B.G. Frederick, *App. Catal. A: Gen.* 477 (2014) 64-74.
- [8] C.A. Teles, R.C. Rabelo-Neto, J.R. Lima, L.V. Mattos, D.E. Resasco, F.B. Noronha, *Catal. Lett.* 146 (2016) 1848-1857.
- [9] P.M. De-Souza, R.C. Rabelo-Neto, L.E.P. Borges, G. Jacobs, B.H. Davis, D.E. Resasco, F.B. Noronha, *ACS Catal.* 7 (2017) 2058-2073.
- [10] L. Nie, P.M. De-Souza, F.B. Noronha, W. An, T. Sooknoi, D.E. Resasco, *J. Mol. Catal. A: Chem.* 388-389 (2014) 47-55.
- [11] Q. Tan, G. Wang, L. Nie, A. Dinse, C. Buda, J. Shabaker, D.E. Resasco, *ACS Catal.* 5 (2015) 6271-6283.
- [12] M.B. Griffin, G.A. Ferguson, D.A. Ruddy, M.J. Bidy, G.T. Beckham, J.A. Schaidle, *ACS Catal.* 6 (2016) 2715-2727.
- [13] T.M. Sankaranarayanan, A. Berenguer, C.O. Hernández, I. Moreno, P. Jana, J.M. Coronado, D.P. Serrano, *Catal. Today* 243 (2015) 163-172.
- [14] T.N. Phan, Y-K. Park, I-G. Lee, C.H. Ko, *App. Catal. A: Gen.* 544 (2017) 84-93.
- [15] M. Hellinger, H.W.P. Carvalho, S. Baier, D. Wang, W. Kleist, J-D. Grunwaldt, *Appl. Catal A: Gen.* 25 (2015) 181-192.
- [16] L. Nie, Peng, X. Zhu, *ChemCatChem* 7 (2018) 1064-1074.
- [17] R.C. Nelson, B. Baek, P. Ruiz, B. Goundie, A. Brooks, M.C. Wheeler, B.G. Frederick, L.C. Grabow, R.N. Austin, *ACS Catal.* 5, 11 (2015) 6509-6523.
- [18] A.M. Barrios, C.A. Teles, P.M. De-Souza, R.C. Rabelo-Neto, G. Jacobs, B.H. Davis, L.E.P. Borges, F.B. Noronha, *Catal. Today* 302 (2018) 115-124.
- [19] L. Nie, D.E. Resasco, *J. Catal.* 317 (2014) 22-29.

- [20] C.A. Teles, R.C. Rabelo-Neto, G. Jacobs, B.H. Davis, D.E. Resasco, F.B. Noronha, *ChemCatChem* 9 (2017) 2850-2863.
- [21] P.M. De-Souza, R.C. Rabelo-Neto, L.E.P. Borges, G. Jacobs, B.H. Davis, T. Sooknoi, D.E. Resasco, F.B. Noronha. *ACS Catal.* 5 (2015) 1318-1239.
- [22] C.A. Teles, P.M. De-Souza, R.C. Rabelo-Neto, M.B. Griffin, C. Mukarakate, K.A. Orton, D.E. Resasco, F.B. Noronha, *App. Catal. B: Environm.* 238 (2018) 38-50.
- [23] C.A. Teles, P.M. De-Souza, A.H. Braga, R.C. Rabelo-Neto, A. Teran, G. Jacobs, D.E. Resasco, F.B. Noronha, *App. Catal. B: Environm.* 249 (2019) 292-305.
- [24] I.T. Ghampson, C. Sepúlveda, A.B. Dongil, G. Pecchi, R. García, J.L.G. Fierro, N. Escalona, *Catal. Sci. Technol.* 6 (2016) 7289-7306.
- [25] Q. Tan, G. Wang, A. Long, A. Dinse, C. Buda, J. Shabaker, D.E. Resasco, *J. Catal.* 347 (2017) 102-115.
- [26] M.A. González-Borja, D.E. Resasco, *Energy Fuels* 25 (2011) 4155-4162.
- [27] S. Leng, X. Wang, X. He, L. Liu, Y.E. Liu, X. Zhong, G. Zhuang, J-G. Wang, *Catal. Commun.* 41 (2013) 34-37.
- [28] T.H. Parsell, B.C. Owen, I. Klein, T.M. Jarrell, C.L. Marcum, L.J. Hauptert, L.M. Amundson, H.I. Kenttamaa, F. Ribeiro, J.T. Miller, *Chem. Science*, 4 (2013) 806-813.
- [29] R.N. Olcese, M. Bettahar, D. Petitjean, B. Malaman, F. Giovanella, A. Dufour, *App. Catal. B: Environm.* 115-116 (2012) 63-73.
- [30] D. Gao, C. Schweitzer, H.T. Hwang, A. Varma, *Ind. Eng. Chem. Res.* 53 (2014) 18658-18667.
- [31] C.R. Lee, J.S. Yoon, Y-W. Choi, J-M. Ha, D.J. Suh, Y-K. Park, *Catal. Commun.* 17 (2012) 54-58.
- [32] Y. Wang, J. Wu, S. Wang, *RCS Adv.* 3 (2013) 12635-12640.

- [33] A. Gutierrez, R.K. Kaila, M.L. Honkela, R. Slioor, A.O.I. Krause, *Catal. Today* 147 (2009) 239-246.
- [34] M.V. Bykova, D.Y. Ermakov, V.V. Kaichev, O.A. Bulavchenko, A.A. Saraev, M.Y. Lebedev, V.A. Yakovlev, *App. Catal. B: Environm.* 113-114 (2012) 296-307.
- [35] X. Zhang, T. Wang, L. Ma, Q. Zhang, Y. Yu, Q. Liu, *Catal. Commun.* 33 (2013) 15-19.
- [36] R. Shu, B. Lin, J. Zhang, C. Wang, Z. Yang, Y. Chen, *Fuel Proc. Technol.* 184 (2019) 12-18.
- [37] S.T. Oyama, T. Onkawa, A. Takagaki, R. Kikuchi, S. Hosokai, Y. Suzuki, K.K. Bando, *Top. Catal.* 58 (2015) 201-210.
- [38] J.E. Peters, J.R. Carpenter, D.C. Dayton, *Energy Fuels* 29 (2015) 909-916.
- [39] X. Xu, E. Jiang, Y. Du, B. Li, *Renew. Energy* 96 (2016) 458-468.
- [40] I. Graça, J.M. Lopes, M.F. Ribeiro, H.S. Cergueira, M.B.B. Almeida, *App. Catal. B: Environm.* 101 (2011) 613-621.
- [41] G.S. Foo, A.K. Rogers, M.M. Yung, C. Sievers, *ACS Catal.* 6 (2016) 1292-1307.
- [42] H.Y. Zhao, D. Li, P. Bui, S.T. Oyama, *App. Catal. A* 391 (2011) 305-310.
- [43] P.M De-Souza, L. Nie, L.E.P. Borges, F.B. Noronha, D.E. Resasco, *Catal. Letters* 144 (2014) 2005-2011.
- [44] S. Boonyasuwat, T. Omotoso, D.E. Resasco, S.P. Crossley, *Catal. Lett.* 143 (2013) 783-791.
- [45] M. Hellinger, H.W.P. Carvalho, S. Baier, D. Wang, W. Kleist, J.D. Grundwaldt, *App. Catal. A* 490 (2015) 181-192.
- [46] W. Song, Y. Liu, E. Barath, C. Zhao, J.A. Lercher, *Green Chem.* 17 (2015) 1204-1218.

- [47] Y-K. Hong, D-W. Lee, H-J. Eom, K-Y. Lee, *App. Catal. B: Environn.* 150-151 (2014) 438-445.
- [48] R. Dang, X. Ma, J. Luo, Y. Zhang, J. Fu, C. Li, N. Yang, *J. Energy Inst.* 93 (2020) 1527-1534.
- [49] C.A. Teles, unpublished doctoral thesis, Military Institute of Engineering, 2019.
- [50] Y. Li, J. Fu, B. Chen, *RSC Adv.* 7 (2017) 15272-15277.
- [51] W. Guan, X. Chen, C. Li, J. Zhang, C-W. Tsang, H. Hu, S. Li, C. Liang, *Mol. Catal.* 467 (2019) 61-69.
- [52] A.A. Dwiatmoko, S. Lee, H.C. Ham, J-W. Choi, D.J. Suh, J-M. Ha, *ACS Catal.* 5 (2015) 433-437.
- [53] Y.C. Lin, C.L. Li, H.P. Wan, H.T. Lee, C.F. Liu, *Energy Fuels* 25 (2011) 890-896.
- [54] T. Nimmanwudipong, R.C. Runnebaum, D.E. Block, B.C. Gates, *Catal. Lett.* 141 (2011) 779-783.
- [55] J. Filley, C. Roth, *J. Mol. Catal. A: Chem* 139 (1999) 245-252.
- [56] D.R. Taylor, K.H. Ludlum, *J. Phys. Chem.* 76 (1972) 2882-2886.
- [57] B-Q. Xu, T. Yamaguchi, K. Tanabe, *Mater. Chem. Phys.* 19 (1988) 291-297.
- [58] T. Mathew, M. Vijayaraj, S. Pai, B.B. Tope, S.G. Hedge, B.S. Rao, CS. Gopinath, *J. Catal.* 227 (2004) 175-185.
- [59] A. Popov, E. Kondratieva, J.M. Goupil, L. Mariey, P. Bazin, J-P. Gilson, A. Travert, F. Maugé, *J. Phys. Chem.* 114 (2010) 15661-15670.
- [60] A. Popov, E. Kondratieva, J-P. Gilson, L. Mariey, A. Travert, *Catal. Today* 172 (2011) 132-135.
- [61] T.M.C. Hoang, N.K. Rao, L. Lefferts, K. Seshan, *ChemCatChem* 7 (2015) 468-478.

- [62] Z. Zhang, X. Hu, L. Zhang, Y. Yang, Q. Li, H. Fan, Q. Liu, T. Wei, C-Z. Li, *Fuel Proc. Technol.* 191 (2019) 138-151.
- [63] J. Chang, T. Danuthai, S. Dewiyanti, C. Wang, A. Borgna, *ChemCatChem* 5 (2013) 3041-3049.
- [64] L. Mariey, J. Lamotte, J.C. Lavalley, N.M. Tsyganenko, A.A Tsyganenko, *Catal. Lett.* 41 (1996) 209-211.
- [65] K. Nakamoto, *Infrared Spectra of Inorganic and Coordination Compounds*, Wiley, New York, 1963, p. 199.
- [66] V.N. Bui, D. Laurenti, P. Afanasiev, C. Geantet, *App. Catal. B: Environm.* 101 (2011) 239-245.
- [67] S-K. Wu, P-C. Lai, Y-C. Lin, H-P. Wan, H-T. Lee, Y-H. Chang, *ACS Sustainable Chem. Eng.* 1 (2013) 349-358.
- [68] Y. Xu, W.K. Chen, S.H. Liu, M.J. Cao, J.Q. Li, *Chem. Phys.* 331 (2007) 275-282.
- [69] H. Fang, J. Zheng, X. Luo, J. Du, A. Roldan, S. Leoni, Y. Yuan, *App. Catal. A: Gen.* 529 (2017) 20-31.
- [70] X. Liu, W. An, Y. Wang, C.H Turner, D.E. Resasco, *Catal. Sci. Technol.* 8 (2018) 2146-2158.
- [71] J. Zhou, W. An, *Catal. Sci. Technol.* doi.org/10.1039/D0CY01361G.
- [72] H-T. Chen, G. Pacchioni. *ChemCatChem* 8 (2016) 2492-2499.
- [73] S.C. Fung, S.J. Tauster, R.L. Garten. *J. Am. Chem. Soc.* 100, (1978) 170-175.
- [74] Q. Fu, T. Wagner, S. Olliges, H-D. Carstanjen. *J.Phys. Chem. B* 109 (2005) 944-951.
- [75] X. Zhao, X. Wu, H. Wang, J. Han, Q. Ge, X. Zhu. *Chem. Select* 3 (2018) 10364-10370.

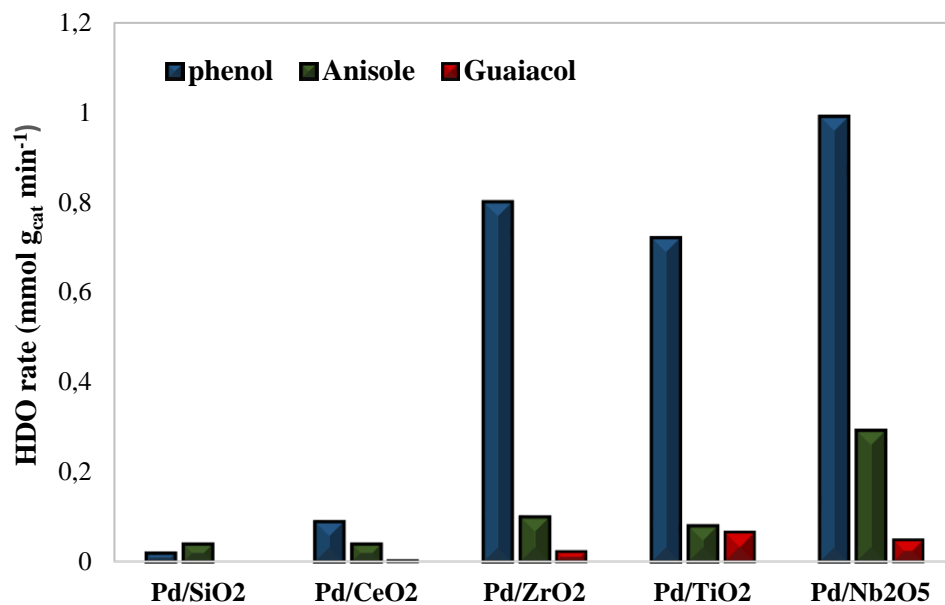


Figure 1. HDO reaction rate for the different catalysts in the HDO reaction of phenol, anisole and guaiacol at gas phase and atmospheric pressure [49].

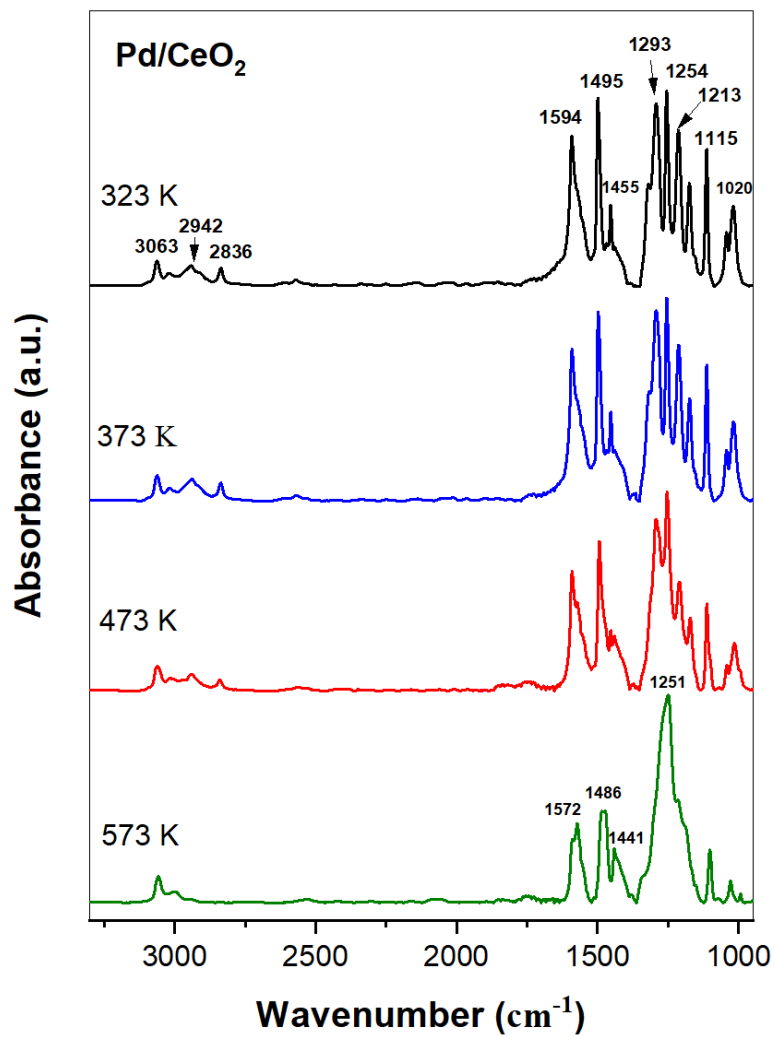


Figure 2. DRIFTS spectra for the TPD of guaiacol in flowing helium at different temperatures for the Pd/CeO₂ catalyst.

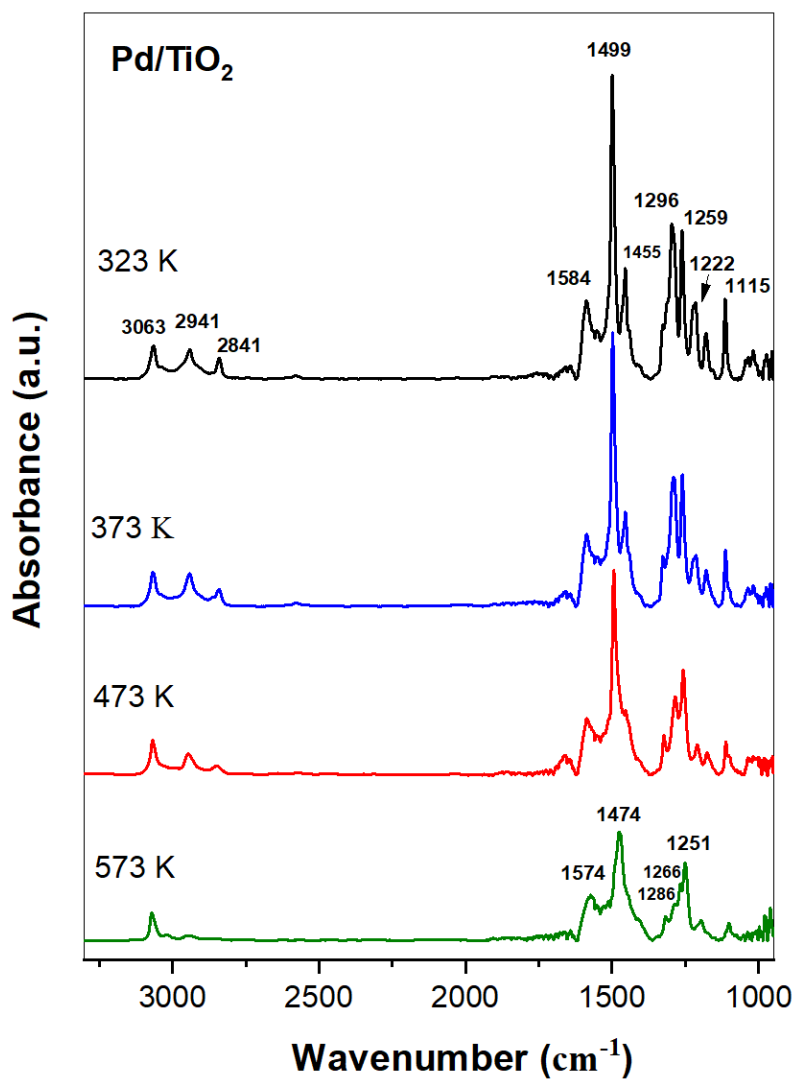


Figure 3. DRIFTS spectra for the TPD of guaiacol in flowing helium at different temperatures for the Pd/TiO₂ catalyst.

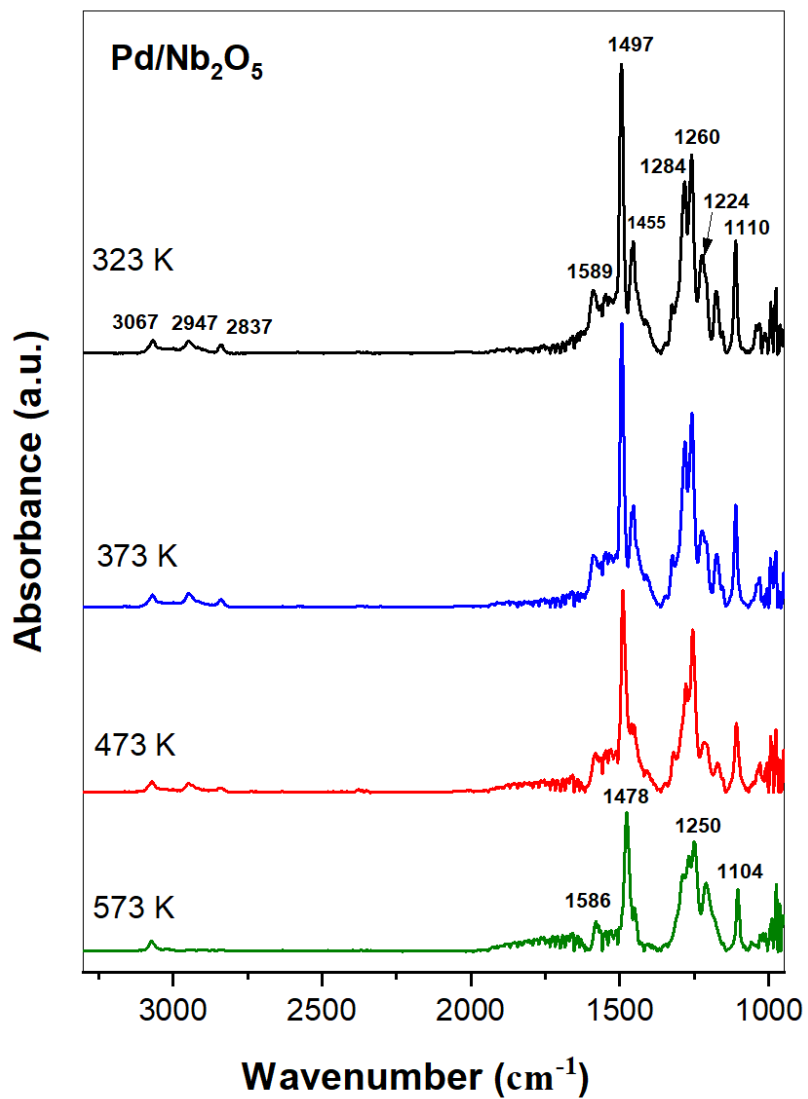


Figure 4. DRIFTS spectra for the TPD of guaiacol in flowing helium at different temperatures for the Pd/Nb₂O₅ catalyst.

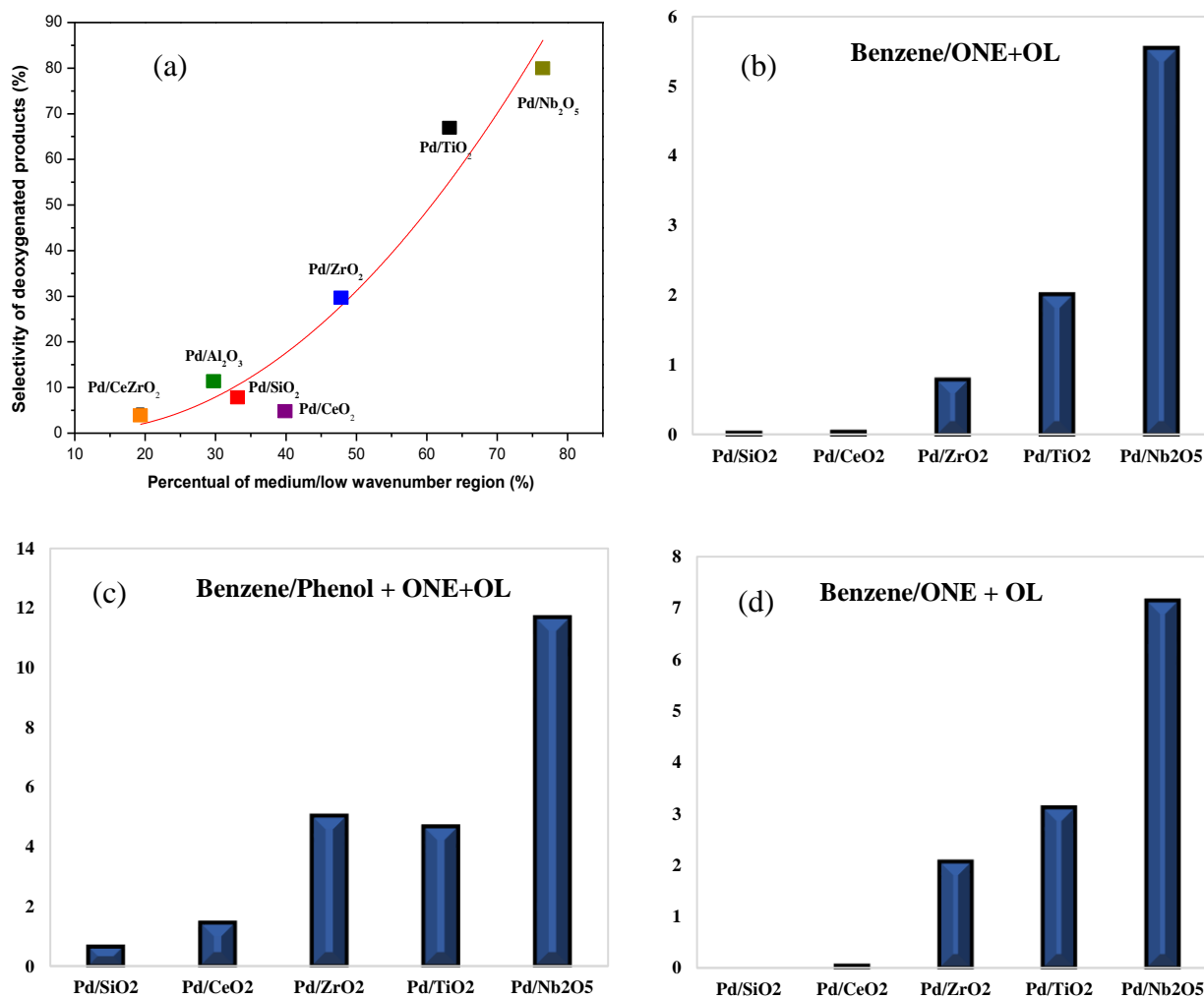


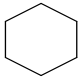
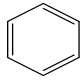
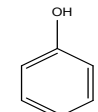
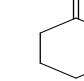
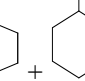
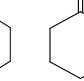
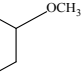
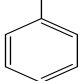
Figure 5. (a) Selectivity to deoxygenated products as a function of the interaction strength between the oxygen from a carbonyl group and the oxophilic cations on the support of catalyst [9]; Deoxygenation/hydrogenation ratio for the different feeds: (b) phenol [49]; (c) anisole [49] and (d) guaiacol.

Table 1. Specific area, Pd dispersion and total amount of ammonia desorbed.

| Catalyst | S (m ² /g) | D ^[a] (%) | Ammonia desorbed (μmol/g _{cat}) |
|-----------------------------------|-----------------------|----------------------|--|
| Pd/SiO ₂ | 153 | 13 | 8 |
| Pd/CeO ₂ | 56 | 27 | 59 |
| Pd/ZrO ₂ | 102 | 70 | 300 |
| Pd/TiO ₂ | 54 | 63 | 225 |
| Pd/Nb ₂ O ₅ | 87 | 22 | 249 |

^[a] Pd dispersion calculated by cyclohexane dehydrogenation reaction for catalyst reduced at 573 K.

Table 2. Conversion, rate of HDO reaction and products distribution for hydrodeoxygenation of guaiacol over the different catalysts ($T_{\text{reaction}} = 573 \text{ K}$, 1 atm).

| Catalyst | Conversion (%) | HDO rate ($\text{mmol g}^{-1}_{\text{cat}} \text{min}^{-1}$) | Selectivity (%) | | | | | | | | | |
|-----------------------------------|----------------|--|---|---|--|---|---|---|---|---|---------------|------------------------|
| | | |  |  |  |  |  |  |  |  | CH_4 | CH_3OH |
| Pd/SiO ₂ | 14.3 | 0.000 | - | - | 41.8 | 4.7 | 0.8 | - | 8.0 | 44.1 | - | 1.1 |
| Pd/CeO ₂ | 9.6 | 0.003 | - | 0.4 | 32.5 | 8.8 | 11.5 | 0.5 | 10.0 | 36.3 | - | 0.9 |
| Pd/ZrO ₂ | 11.1 | 0.022 | 0.3 | 15.0 | 22.7 | 7.4 | 2.8 | 5.4 | 21.2 | 23.6 | 1.6 | 1.0 |
| Pd/TiO ₂ | 15.5 | 0.063 | - | 13.4 | 26.8 | 4.3 | 2.0 | 7.5 | 7.6 | 38.1 | 0.3 | 1.0 |
| Pd/Nb ₂ O ₅ | 25.0 | 0.047 | 0.5 | 15.7 | 27.1 | 2.2 | 3.0 | 8.7 | 8.4 | 31.7 | 2.7 | 1.0 |

Others*: methoxy-cyclohexane, o-cresol, m-cresol and biphenyl.

** Ratio of the yield of C1 (methane and methanol) and C6 (cyclohexane, benzene, cyclohexanone, cyclohexanol).

Table 3. Vibrational mode assignment of the bands in DRIFTS spectra recorded for the different model molecules on different materials.

| Assignment | Phenol | | | Anisole | | | Guaiacol | | |
|--|--|--|--|--|--|--|--|--|--------------------------|
| | Pd/CeO ₂ , Pd/Al ₂ O ₃ , Pd/ZrO ₂ , Pd/TiO ₂ [9] | Pd/CeO ₂ , Pd/ZrO ₂ , Pd/TiO ₂ [49] | Al ₂ O ₃ [59] | Pd/CeO ₂ , Pd/ZrO ₂ , Pd/TiO ₂ [49] | CuCoFe ₂ O ₄ [58] | Al ₂ O ₃ [59] | Ni/Al ₂ O ₃ , Ni/SBA-15 [62] | Al ₂ O ₃ [59] | MoO ₃ [63] |
| $\nu(\text{C-H}_{\text{ring}})$ | 3054-3065 | 3050-3069 | -- | 2940-3075 | 3008-3062 | -- | -- | -- | -- |
| $\nu(\text{CH}_2/\text{CH}_3)$ | 2931-2859 | 2930-2947 | -- | 2775-2844 | 2922-2840 | -- | -- | -- | -- |
| $\nu(\text{C}=\text{C}_{\text{ring}})$ | 1591-1594 | 1587-1594 | 1597 | 1593-1599 | 1594 | 1593 | 1590 | 1597 | 1610 |
| $\nu(\text{C}=\text{C}_{\text{ring}})$ | 1491-1495 | 1482-1496 | 1498 | 1494-1499 | 1493 | 1490 | 1450 | 1497 | 1512 |
| $\delta(\text{CH}_3)$ | -- | -- | -- | 1454 | 1460 | 1458 | -- | 1460 | -- |
| $\nu(\text{C}_{\text{Ar}}-\text{OH})$ | 1262-1291 | 1260, 1286 | 1250, 1295 | -- | -- | -- | -- | 1260 | 1271 |
| $\nu(\text{C}_{\text{Ar}}-\text{OCH}_3)$ | -- | -- | -- | 1245, 1296 | 1242, 1290 | 1248, 1295 | 1277 | 1225 | 1234 |
| $\nu(\text{H}_3\text{C}-\text{O})$ | -- | -- | -- | 1035-1114 | 1000-1080 | | 1100 | -- | 1100 |

